PHYSICAL REVIEW B **79**, 220509(R) (2009)

Quantum critical behavior driven by Hund's rule coupling in quantum antiferromagnets

Efstratios Manousakis
Department of Physics and MARTECH, Florida State University, Tallahassee, Florida 32306-4350, USA
and Department of Physics, University of Athens, Panepistimioupolis, Zografos, 157 84 Athens, Greece
(Received 5 March 2009; revised manuscript received 24 April 2009; published 19 June 2009)

When localized spins on different d orbitals prefer different types of antiferromagnetic ordering, the Hund's rule coupling creates frustration. Using spin-wave theory we study the case of two such orbitals on a square lattice coupled through Hund's rule such that the first one couples antiferromagnetically more strongly to its nearest neighbors, while the second couples more strongly to its next nearest neighbors. We find that the zero temperature phase diagram has four regions: one characterized by the familiar (π,π) antiferromagnetic order, a second by the columnar $(\pi,0)$ order, a third by a *canted* order, and a fourth region where a quantum-disordered state emerges. We comment on the possible relevance of these findings for the case of Fe-pnictide-based antiferromagnets.

DOI: 10.1103/PhysRevB.79.220509 PACS number(s): 74.70.−b, 75.10.Jm, 75.30.Ds, 75.40.Gb

The FeAs layer of the parent compound of the Fe-pnictide superconductors[1] below approximately 134 K undergoes a spin-density-wave (SDW) ordering with a small magnetic moment $\sim 0.35\mu_B$ per Fe atom.[2,3] The d orbitals of the Fe atom are occupied by several electrons; and in the limit where the Hund's rule coupling is large compared to the nearest-neighbor (NN) and next nearest-neighbor (NNN) antiferromagnetic couplings, which is believed to be the case for these materials, we may expect a much larger moment[4–7] per Fe atom ($\sim 2.6\mu_B$). Even though other similar materials show higher values of the Fe moment[11] the small value of the observed magnetic moment, as well as other considerations, has fueled a belief that the magnetism in these materials may be of itinerant type.[8–10] In the present Rapid Communication we explore the possibility that the origin of this significantly reduced moment is a result of frustration introduced by the fact that the various Fe d orbitals prefer a different and competing type of magnetic ordering.

First, let us consider a simplified model in order to introduce the reader to the problem discussed here and in order to overview our main findings. The more realistic model,[12] treated within the spin-wave theory (SWT), will be presented below. The Hamiltonian,

$$\mathcal{H} = J_1 \sum_{\langle ij \rangle} \mathbf{S}_i^1 \cdot \mathbf{S}_j^1 + J_2 \sum_{\langle\langle ij \rangle\rangle} \mathbf{S}_i^2 \cdot \mathbf{S}_j^2 - J_H \sum_i \mathbf{S}_i^1 \cdot \mathbf{S}_i^2, \qquad (1)$$

describes two distinct spin operators $\mathbf{S}_i^1$ and $\mathbf{S}_i^2$ corresponding to two different d orbitals of the same ith Fe atom. The spins $\mathbf{S}_i^1$ interact antiferromagnetically with their NN $\mathbf{S}_j^1$, while the spins $\mathbf{S}_i^2$ interact with their NNN $\mathbf{S}_j^2$ (along the diagonal of the square). The Hund's rule coupling J_H tends to align the spins on the same atom. The origin of qualitatively different spin interactions for two different d orbitals is discussed in Ref. 12. When $J_H=0$, the spins $\mathbf{S}_i^1$ order in the (π,π) order indicated by the horizontally aligned (red) spins in Fig. 1(a), while the spins $\mathbf{S}_i^2$ order in the $(\pi,0)$ [or $(0,\pi)$] order indicated by the blue-colored spins in Fig. 1(a). In the absence of J_H any choice of direction of order for either type of spins is equally acceptable because our model is rotationally symmetric. When $J_H>0$ the canted state of Fig. 1(b) is obtained as a compromise state between the two extremes of Fig. 1(a) by tilting the orientation of the vertically aligned (blue) spins by an angle ϕ toward the red and the horizontally aligned spins toward the orientation of the vertically aligned spins by an angle θ. The two spins "bend" toward each other due to Hund's rule coupling. Through this canting there is some gain from the term proportional to J_H and some loss due to both types of spin-spin interactions. When J_1 is not too different from $2J_2$ (see Fig. 2), the classical ground state is the canted state of Fig. 1(b) for any value of J_H.

In this Rapid Communication we also study the role of quantum fluctuations around the classical ground states within SWT. We find large amplitude quantum spin fluctuations when J_1 is sufficiently close to $2J_2$ and near or in the canted phase. Further, we find that for sufficiently large

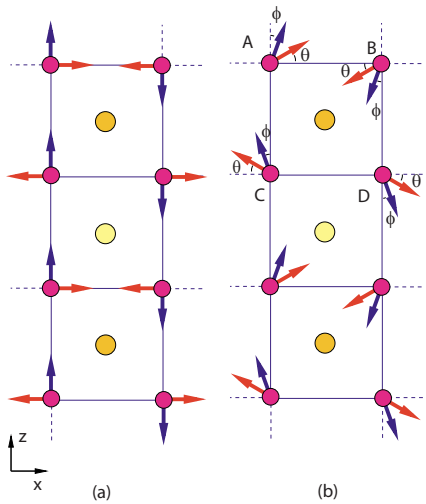

FIG. 1. (Color online) The classical ground state of the Hamiltonian given by Eq. (3). The circles at the vertices of each square denote Fe atoms. The circles at the center of each square denote As atoms. (a) $J_H \to 0$: the horizontally aligned spins are described by $\mathcal{H}^{(1)}$ and they prefer the (π,π) state, while the vertically aligned spins are described by $\mathcal{H}^{(2)}$ and prefer the columnar order. (b) The canted state: the J_H term rotates the spins toward each other by angles θ and ϕ.

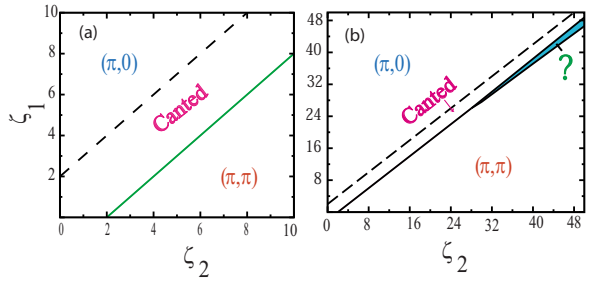

FIG. 2. (Color online) (a) The classical phase diagram. (b) The phase diagram as determined by the SWT. In the region labeled by a question mark the magnetic order is destroyed.

J_H/J_1 (and J_H/J_2) there is a quantum critical point near $J_H/J_1 \sim J_H/(2J_2)-4$ (taking $S_1=S_2$) from where a region of a quantum-disordered state begins. We discuss the consequences of our findings for the magnetic state of the Fe pnictides and possible future neutron-scattering experiments to search for the canted and the disordered states. The simpler well-known J_1-J_2 model[13–15] is obtained from our model in the limit of very large J_H. However, in order to explain the observed reduced moment, the J_1-J_2 model requires fine tuning of the J_1/J_2 ratio to a value very close to the quantum critical point; on the contrary, the present model has a much broader parameter range yielding large amplitude quantum spin fluctuations necessary to explain the observed reduced moment in the Fe pnictides.

The problem to be discussed here is a somewhat simplified version of the general Hamiltonian derived in Ref. 12 and a generalization of the Hamiltonian given by Eq. (1),

$$\mathcal{H} = \sum_{\nu} \mathcal{H}^{(\nu)} - J_H \sum_{i,\nu\neq\nu'} \mathbf{S}_i^{\nu}\cdot\mathbf{S}_i^{\nu'}, \tag{2}$$

$$\mathcal{H}^{(\nu)} = J_1^{(\nu)} \sum_{\langle ij\rangle} \mathbf{S}_i^{\nu}\cdot\mathbf{S}_j^{\nu} + J_2^{(\nu)} \sum_{\langle\langle ij\rangle\rangle} \mathbf{S}_i^{\nu}\cdot\mathbf{S}_j^{\nu}, \tag{3}$$

where the index $\nu=1,2,\ldots,5$ refers to the five Fe d orbitals. When we consider each of the parts $\mathcal{H}^{(\nu)}$ separately, if $J_2^{(\nu)} > J_1^{(\nu)}/2$, the $(\pi,0)$ order [blue-colored spins of Fig. 1(a)] is stable; otherwise within SWT, the (π,π) antiferromagnetic order [red-colored spins in Fig. 1(a)] takes over. For some of the Fe d orbitals in the FeAs-based materials $J_2^{(\nu)} > J_1^{(\nu)}/2$, while for other d orbitals this condition is not satisfied.[12] We have carried out the SWT calculation including all five Fe d orbitals; however, this Hamiltonian has ten independent parameters; and, thus, it is hard to present the results for the entire parameter space. For simplicity, we will present here the case of just two orbitals such that the first one, i.e., $\nu=1$, satisfies the condition $J_2^{(1)} < J_1^{(1)}/2$ for (π,π) order, while the $\nu=2$ orbital satisfies the condition $J_2^{(1)} > J_1^{(1)}/2$ for the $(\pi,0)$ order. As discussed above we are interested in the case where one spin flavor prefers the columnar $[(0,\pi)]$ order and the other the antiferromagnetic $[(\pi,\pi)]$ order. We find that presenting the results for just two orbitals is clear and cleaner, and the qualitative results and conclusions are the same with the main results of the more general Hamiltonian described by Eq. (3). However, we have generalized the spin-1/2 operators to spin-S case in order to capture some of the physics of the more-than-two orbital case.

First, notice that the Hamiltonian at the classical level for certain range of the coupling constants has a ground state shown in Fig. 1(b). The blue spins of the up sublattice are canted by an angle ϕ and the red spins by an angle θ as shown in the figure. The total energy difference from the energy of the state of Fig. 1(a) is $\delta E = -\frac{\alpha_1}{2}\cos(2\theta) - \frac{\alpha_2}{2}\cos(2\phi) - J_H S_1 S_2 \sin(\theta+\phi)$, where $\alpha_1 = 2S_1^2(J_1^{(1)} - 2J_2^{(1)})$, $\alpha_2 = 2S_2^2(2J_2^{(2)} - J_1^{(2)})$, and $S_{1,2}$ are the maximum length of the two classical spins. In the interval $0 \le \theta \le \pi/2$ and $0 \le \phi \le \pi/2$, there are the following extrema of the energy. First, the following two trivial solutions $(\theta,\phi) = (\frac{\pi}{2},0)$ and $(\theta,\phi) = (0,\frac{\pi}{2})$, each of which is a stable absolute minimum, respectively, when $\zeta_1 - \zeta_2 > 2$ and $\zeta_2 - \zeta_1 > 2$, where $\zeta_\nu = \frac{S_1 S_2 J_H}{\alpha_\nu}$. When neither of these conditions for trivial solutions is satisfied the stable absolute minimum is given by

$$\sin^2(2\phi) = \zeta_2^2 \frac{1 - \left(\frac{\zeta_1 - \zeta_2}{2}\right)^2}{1 + \zeta_1\zeta_2}, \quad \sin(2\theta) = \frac{\zeta_1}{\zeta_2}\sin(2\phi). \tag{4}$$

The classical phase diagram is shown in Fig. 2(a). Notice that for any value of the J_H there is the canted phase with the angles given as in Eq. (4) provided that the other couplings α_1 and α_2 are not very different from each other, i.e., when they satisfy the condition discussed above. If, however, these couplings are very different in magnitude, the global ground state is the one preferred by the stronger coupling; i.e., if $\alpha_2 \gg \alpha_1$ the $(\pi,0)$ order is the ground state, and when $\alpha_1 \gg \alpha_2$ the (π,π) state wins. Both transition lines separating the canted order from the (π,π) order, or from the $(\pi,0)$ order, are lines of second-order critical points.

In order to study the role of quantum fluctuations, we first carry out a local rotation of the spin quantization axes along the direction of the classical order, i.e., by angles θ and ϕ for spins on sublattice A as follows: $S_i^{1z'} = \sin\theta S_i^{1z} - \cos\theta S_i^{1x}$ and $S_i^{1x'} = \cos\theta S_i^{1z} + \sin\theta S_i^{1x}$, while the y component remains unchanged because we have assumed that the rotation is in the x-z plane (the plane of the drawing). The expressions for the second type spin are obtained from the above by replacing $\theta \to \pi/2 - \phi$. For sublattices B, C, and D, we can still use the above expressions but with the angles (ϕ,θ) replaced by $(\pi+\phi,\pi+\theta)$, $(\pi-\phi,-\theta)$, and $(-\phi,\pi-\theta)$, respectively.

In order to apply the SWT,[16] we express the operators $S_i^{\nu z}$ and $S_i^{\nu x} S_i^{\nu y}$ using the spin-deviation operators, i.e., $S_i^{\nu z} = S_\nu - a_{i,\nu}^\dagger a_{i,\nu}$, $S_i^{\nu x} = \sqrt{\frac{S_\nu}{2}}(a_{i,\nu}^\dagger + a_{i,\nu})$, and $S_i^{\nu y} = i\sqrt{\frac{S_\nu}{2}}(a_{i,\nu}^\dagger - a_{i,\nu})$, for both cases of spin "color" $\nu=1,2$. By substituting these operators in the Hamiltonian given by Eq. (3), and keeping up to quadratic terms in spin-deviation operators we obtain

$$\mathcal{H} = E_0 + \sum_{\nu,\mathbf{k}} \left[A_{\mathbf{k}}^{(\nu)} a_{\mathbf{k},\nu}^\dagger a_{\mathbf{k},\nu} + \frac{B_{\mathbf{k}}^{(\nu)}}{2}(a_{\mathbf{k},\nu}^\dagger a_{-\mathbf{k},\nu}^\dagger + \text{H.c.}) \right] + \sum_{\mathbf{k}} (V_{\mathbf{k}} a_{\mathbf{k},1}^\dagger a_{\mathbf{k},2} + \text{H.c.} + W_{\mathbf{k}} a_{\mathbf{k},1}^\dagger a_{-\mathbf{k},2}^\dagger + \text{H.c.}), \tag{5}$$

where

TABLE I. The factors needed in Eqs. (6) and (7) are given below. The notation $c_x=\cos k_x$, $c_y=\cos k_y$, and $c_{xy}=\cos k_x \cos k_y$ is used.

(ν,μ)	$f_\mu^{(\nu)}$	$g_\mu^{(\nu)}$
(1,1)	$2S_1[2\cos^2(\theta)+c_y\sin^2(\theta)]$	$-2S_1[c_x+c_y\cos^2(\theta)]$
(1,2)	$4S_1[\cos^2(\theta)c_{xy}-\cos(2\theta)]$	$-4S_1\sin^2(\theta)c_{xy}$
(2,1)	$2S_2[2\sin^2(\phi)+\cos^2(\phi)c_y]$	$-2S_2[c_x+c_y\sin^2(\phi)]$
(2,2)	$4S_2[\cos(2\phi)+c_{xy}\sin^2(\phi)]$	$-4S_2\cos^2(\phi)c_{xy}$

$$A_{\mathbf{k}}^{(\nu)}=J_1^{(\nu)}f_1^{(\nu)}+J_2^{(\nu)}f_2^{(\nu)}+J_Hc_H^{(\nu)}, \tag{6}$$

$$B_{\mathbf{k}}^{(\nu)}=J_1^{(\nu)}g_1^{(\nu)}+J_2^{(\nu)}g_2^{(\nu)}, \quad c_H^{(\nu)}=\bar{S}_\nu\sin(\phi+\theta), \tag{7}$$

$\bar{S}_\nu=S_1S_2/S_\nu$, and f_i^ν and g_i^ν are given in Table I.

$$V_{\mathbf{k}}=-\xi(1+\sin(\phi+\theta)), \quad W_{\mathbf{k}}=\xi(1-\sin(\phi+\theta)), \tag{8}$$

where $\xi=J_H\sqrt{S_1S_2}/2$ and $a_{\mathbf{k},\nu}$ are the Fourier components of the operators $a_{i,\nu}$ defined over the entire Brillouin zone (BZ) of the nonmagnetically ordered system; i.e., $-\pi<k_x,k_y\leq\pi$ (in our units the lattice spacing $a=1$).

There are terms proportional to $(S_i^{\nu z}S_j^{\nu x}-S_i^{x\nu}S_j^{z\nu})$ arising from both the $\mathcal{H}^{(\nu)}$ and the J_H terms. In the SWT, they lead to linear terms in the operators $a_{i,\nu}$ and $a_{i,\nu}^\dagger$ which can be eliminated by choosing the angles to be those minimizing the classical energy.

Now, the quadratic Hamiltonian given by Eq. (5) can be diagonalized by means of a canonical transformation,

$$a_{\mathbf{k},\nu}=\sum_{\mu=1}^{2}[u_{\mathbf{k},\nu}^{(\mu)}\alpha_{\mathbf{k},\mu}+v_{\mathbf{k},\nu}^{(\mu)}\alpha_{-\mathbf{k},\mu}^\dagger], \tag{9}$$

where the coefficients should be chosen to preserve the canonical commutation relations for the boson operators. This requires the following normalization condition $\Sigma_{\mu=1}^2[|u_{\mathbf{k},\nu}^{(\mu)}|^2-|v_{\mathbf{k},\nu}^{(\mu)}|^2]=1$. Due to the above condition, the requirement for the canonical transformation to transform Hamiltonian (5) in a diagonal form,

$$\mathcal{H}=C+\sum_{\nu=1}^{2}\omega_{\mathbf{k}\nu}\left(\alpha_{\mathbf{k},\nu}^\dagger\alpha_{\mathbf{k},\nu}+\frac{1}{2}\right), \tag{10}$$

implies that the eigenfrequencies $\omega_{\mathbf{k},\nu}$ and eigenvectors $\alpha_{\mathbf{k},\nu}^\dagger$ are given from the set of equations $D(\omega_{\mathbf{k},\nu})\mathbf{x}^{(\nu)}=0$, where the matrix

$$D(\omega)\equiv\begin{pmatrix} A_{\mathbf{k}}^{(1)}-\omega & B_{\mathbf{k}}^{(1)} & V_{\mathbf{k}} & W_{\mathbf{k}} \\ B_{\mathbf{k}}^{(1)} & A_{\mathbf{k}}^{(1)}+\omega & W_{\mathbf{k}} & V_{\mathbf{k}} \\ V_{\mathbf{k}} & W_{\mathbf{k}} & A_{\mathbf{k}}^{(2)}-\omega & B_{\mathbf{k}}^{(2)} \\ W_{\mathbf{k}} & V_{\mathbf{k}} & B_{\mathbf{k}}^{(2)} & A_{\mathbf{k}}^{(2)}+\omega \end{pmatrix} \tag{11}$$

and the components of the vector $\mathbf{x}^{(\nu)}$ are $u_{\mathbf{k},1}^{(\nu)}$, $v_{\mathbf{k},1}^{(\nu)}$, $u_{\mathbf{k},2}^{(\nu)}$, and $v_{\mathbf{k},2}^{(\nu)}$. Here, we have taken advantage of the relations $(u_{-\mathbf{k},\mu}^{(\nu)})^*=u_{\mathbf{k},\mu}^{(\nu)}$ and $(v_{-\mathbf{k},\mu}^{(\nu)})^*=v_{\mathbf{k},\mu}^{(\nu)}$. We find that

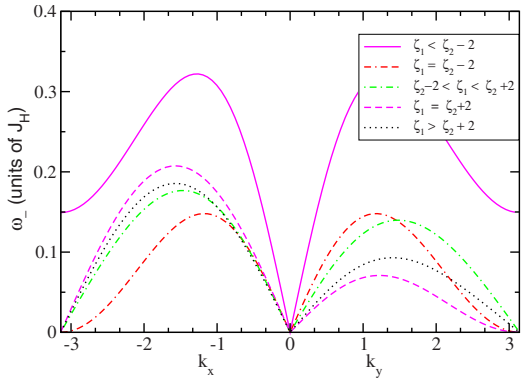

FIG. 3. (Color online) The lowest ("acoustic") spin-wave frequency band along the k_x (negative part of the x axis) and k_y (positive part of the x axis) directions for various values of ζ_1 which correspond to the (π,π) order, the canted phase, and the $(\pi,0)$ order. These results were obtained using $\zeta_2=4$ and $\zeta_1=1,2,3,4,6,8$.

$$\omega_{\mathbf{k},\nu}^2=\Omega_{\mathbf{k}}\pm\sqrt{\Delta_{\mathbf{k}}}, \tag{12}$$

where $\Omega_{\mathbf{k}}=(\eta_{\mathbf{k},1}^2+\eta_{\mathbf{k},2}^2)/2+V_{\mathbf{k}}^2-W_{\mathbf{k}}^2$, $\eta_{\mathbf{k},\nu}^2=(A_{\mathbf{k}}^{(\nu)})^2-(B_{\mathbf{k}}^{(\nu)})^2$, and $\Delta_{\mathbf{k}}=[(\eta_{\mathbf{k},1}^2-\eta_{\mathbf{k},2}^2)/2]^2+(\eta_{\mathbf{k},1}^2+\eta_{\mathbf{k},2}^2)(V_{\mathbf{k}}^2-W_{\mathbf{k}}^2)+2[A_{\mathbf{k}}^{(1)}A_{\mathbf{k}}^{(2)}+B_{\mathbf{k}}^{(1)}B_{\mathbf{k}}^{(2)}](V_{\mathbf{k}}^2+W_{\mathbf{k}}^2)-4[A_{\mathbf{k}}^{(1)}B_{\mathbf{k}}^{(2)}+A_{\mathbf{k}}^{(2)}B_{\mathbf{k}}^{(1)}]V_{\mathbf{k}}W_{\mathbf{k}}$. The staggered magnetizations along the direction of the rotated local coordinate system (by the angles θ and ϕ) are given by

$$m_\nu^\dagger=S_\nu-\frac{1}{N}\sum_{\mathbf{k}}\sum_{\mu=1}^{2}|v_{\mathbf{k},\nu}^{(\mu)}|^2. \tag{13}$$

In the following discussion and calculations presented in the figures we restrict ourselves to the special case where $J_2^{(1)}=J_1^{(2)}=0$ and, thus, $\zeta_1=(S_2J_H)/(2S_1J_1^{(1)})$ and $\zeta_2=(S_1J_H)/(4S_2J_2^{(2)})$. In the entire nonmagnetic BZ, there are two spin-wave frequencies, an "acoustic" branch, i.e., the $\omega_{\mathbf{k},-}$ which vanishes in the long-wavelength limit and the "optical" branch $\omega_{\mathbf{k},+}$ which is constant in the long-wavelength limit and of high energy. The acoustic frequencies are shown in Fig. 3 along the k_x and k_y directions keeping the value of ζ_2 constant at $\zeta_2=4$ and varying the parameter ζ_1. For $\zeta_2=4$ there are two critical values of ζ_1, namely, $\zeta_1^-=2$ and $\zeta_1^+=6$ which define the region of the canted phase. The spin-wave velocities along the two directions for $\zeta_1>\zeta_2-2$ are different as expected.

Notice that at the critical point ζ_1^- where we enter the canted order from the (π,π) order, the modes at the wave vectors $(\pi,0)$ and $(0,\pi)$ (Fig. 3) become soft. We note that in the pure NN antiferromagnet these modes have maximum frequency. At the critical point $\zeta_1=\zeta_1^+$, i.e., at the border between the canted phase and the $(\pi,0)$ phase, these two modes have zero frequency.

In Fig. 4 we present the staggered magnetizations $m_1^\dagger$ and $m_2^\dagger$ along the direction of order for spin $S_1=S_2=1/2$. The various lines are obtained by keeping ζ_2 fixed and by varying ζ_1. Notice that while the magnitude of the staggered magnetization along the rotated direction is a continuous function across the transition to the canted phase, there are singularities in its derivative at $\zeta_1=\zeta_1^\pm=\zeta_2\pm2$. These singularities

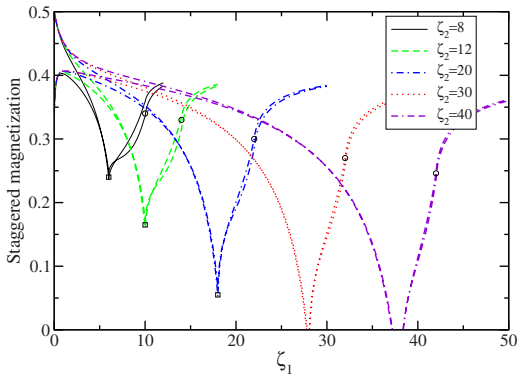

FIG. 4. (Color online) Comparison of staggered magnetizations $m_1^\dagger$ (the lines which start from ~0.5 in the limit of small ζ_1) and $m_2^\dagger$ for spin $S_1=S_2=1/2$ and for various values of ζ_2 as a function of ζ_1.

indicated by the open circles and open squares are caused by the singularities in the abrupt change in the angles θ and ϕ.

Notice that for large-enough ζ_2 and for comparable value of ζ_1 the staggered magnetization along the local polarization axes becomes very small. For large values of ζ_1 the minimum occurs at ζ_1 the boundary between the canted and the (π,π) phase. There is a quantum critical point which is attained when the Hund's rule coupling is large compared to both $J_2^{(2)}$ and $J_1^{(1)}$. This limit is believed to be the case for the Fe pnictides. Our model reduces to the familiar J_1-J_2 model in the limit of $J_H \to \infty$; however, as Fig. 4 indicates reaching this limit requires unrealistically large values of J_H as compared to all other couplings. Notice that the transition to the canted phase from the side of the $(\pi,0)$ order occurs before the staggered magnetization $m_2^\dagger$ becomes small, even for large values of J_H. We find that the reason for the enhancement of quantum fluctuations near the $\zeta_1=\zeta_2-2$ boundary is that the spin-wave velocity for large J_H decreases as we increase $J_H/J_1^{(1)}$, and this is not the case at the $\zeta_1=\zeta_2+2$ boundary. Therefore, there is a quantum-disordered phase shown by the green area in Fig. 2(b) which illustrates the phase diagram as modified by quantum fluctuations.

In neutron diffraction from the FeAs-based antiferromagnets, the canted state should produce a peak with intensity proportional to $\cos^2\phi$ at $\mathbf{k}=(\pi,0)$ [or $(0,\pi)$] which has been observed[2] and a peak with low intensity proportional to $\sin^2\phi$ at $\mathbf{k}=(0,\pi)$ [or $(\pi,0)$]. Therefore, if the canting angle ϕ is small, the latter peak might be more difficult to resolve, and this requires further detailed experimental investigation. In addition, the magnetic unit cell of the FeAs plane of the canted phase is the same as the structural unit cell. This is so because there is an orthorhombic lattice distortion below 155 K and, further, the As atoms are above and below the plane formed by the Fe atoms in a checkerboard pattern. Therefore, diffraction using polarized neutrons might be a simple way to probe this canted phase. The spin-wave dispersion, which is probed by inelastic scattering experiments,[17,18] has no distinctly different features from that of the $(\pi,0)$ phase (see Fig. 4).

The properties of the quantum-disordered state which emerges from the destruction of the long-range order cannot be investigated by the present SWT approach. As found in Refs. 6, 7, 12, 19, and 20, the values of $J_1^{(\nu)}$ and $J_2^{(\nu)}$ are comparable, and therefore this phase may be accessible by altering these parameters experimentally using pressure or electron/hole doping.

In summary, using SWT we found that the model introduced here to describe the magnetic properties of the Fe pnictides has four phases. In addition, to the familiar (π,π) and $(0,\pi)$ phases there is a canted phase and a quantum spin-disordered phase. We have suggested that the canted phase could be investigated by neutron diffraction by looking for a low intensity peak in a direction orthogonal to that of the main magnetic peak.

[1] Y. Kamihara, T. Watanabe, M. Hirano, and H. Hosono, J. Am. Chem. Soc. **130**, 3296 (2008).
[2] C. de la Cruz, Q. Huang, J. W. Lynn, J. Li, W. Ratcliff II, J. L. Zarestky, H. A. Mook, G. F. Chen, J. L. Luo, N. L. Wang, and P. Dai, Nature (London) **453**, 899 (2008).
[3] H.-H. Klauss, H. Luetkens, R. Klingeler, C. Hess, F. J. Litterst, M. Kraken, M. M. Korshunov, I. Eremin, S.-L. Drechsler, R. Khasanov, A. Amato, J. Hamann-Borrero, N. Leps, A. Kondrat, G. Behr, J. Werner, and B. Buchner, Phys. Rev. Lett. **101**, 077005 (2008).
[4] D. J. Singh and M.-H. Du, Phys. Rev. Lett. **100**, 237003 (2008).
[5] C. Cao, P. J. Hirschfeld, and H.-P. Cheng, Phys. Rev. B **77**, 220506(R) (2008).
[6] T. Yildirim, Phys. Rev. Lett. **101**, 057010 (2008).
[7] F. Ma, Z.-Y. Lu, and T. Xiang, Phys. Rev. B **78**, 224517 (2008).
[8] S. Raghu, X.-L. Qi, C.-X. Liu, D. J. Scalapino, and S.-C. Zhang, Phys. Rev. B **77**, 220503(R) (2008).
[9] A. V. Chubukov, D. V. Efremov, and I. Eremin, Phys. Rev. B **78**, 134512 (2008).
[10] V. Cvetkovic and Z. Tesanovic, EPL **85**, 37002 (2009).
[11] W. Bao, Y. Qiu, Q. Huang, M. A. Green, P. Zajdel, M. R. Fitzsimmons, M. Zhernenkov, M. Feng, B. Qian, E. K. Vehstedt, J. Yang, H. M. Pham, L. Spinu, and Z. Q. Mao, arXiv:0809.2058 (unpublished).
[12] E. Manousakis, J. Ren, S. Meng, and E. Kaxiras, Phys. Rev. B **78**, 205112 (2008); arXiv:0902.3450 (unpublished).
[13] S. Sachdev, *Quantum Phase Transitions* (Cambridge University Press, Cambridge, UK, 1999).
[14] C. Xu, M. Muller, and S. Sachdev, Phys. Rev. B **78**, 020501(R) (2008).
[15] D.-X. Yao and E. W. Carlson, Phys. Rev. B **78**, 052507 (2008).
[16] E. Manousakis, Rev. Mod. Phys. **63**, 1 (1991).
[17] J. Zhao, D.-X. Yao, S. Li, T. Hong, Y. Chen, S. Chang, W. Ratcliff, J. W. Lynn, H. A. Mook, G. F. Chen, J. L. Luo, N. L. Wang, E. W. Carlson, J. Hu, and P. Dai, Phys. Rev. Lett. **101**, 167203 (2008).
[18] R. A. Ewings, T. G. Perring, R. I. Bewley, T. Guidi, M. J. Pitcher, D. R. Parker, S. J. Clarke, and A. T. Boothroyd, Phys. Rev. B **78**, 220501(R) (2008).
[19] J. Dong, H. J. Zhang, G. Xu, Z. Li, G. Li, W. Z. Hu, D. Wu, G. F. Chen, X. Dai, J. L. Luo, Z. Fang, and N. L. Wang, EPL **83**, 27006 (2008).
[20] Z. P. Yin, S. Lebégue, M. J. Han, B. P. Neal, S. Y. Savrasov, and W. E. Pickett, Phys. Rev. Lett. **101**, 047001 (2008).